International Journal of Ambient Energy

ISSN: 0143-0750 (Print) 2162-8246 (Online) Journal homepage: http://www.tandfonline.com/loi/taen20

# Comparative analysis of three numerical methods for estimating the onshore wind power in a coastal area

**Mojtaba Nedaei, Abtin Ataei, Muyiwa Samuel Adaramola, Alireza Hajiseyed Mirzahosseini, Morteza Khalaji Assadi & Ehsanolah Assareh**

**To cite this article:** Mojtaba Nedaei, Abtin Ataei, Muyiwa Samuel Adaramola, Alireza Hajiseyed Mirzahosseini, Morteza Khalaji Assadi & Ehsanolah Assareh (2016): Comparative analysis of three numerical methods for estimating the onshore wind power in a coastal area, International Journal of Ambient Energy, DOI: 10.1080/01430750.2016.1237890

**To link to this article:** http://dx.doi.org/10.1080/01430750.2016.1237890

Accepted author version posted online: 16 Sep 2016.
Published online: 30 Sep 2016.

INTERNATIONAL JOURNAL OF AMBIENT ENERGY, 2016
http://dx.doi.org/10.1080/01430750.2016.1237890

Taylor & Francis
Taylor & Francis Group

# Comparative analysis of three numerical methods for estimating the onshore wind power in a coastal area

Mojtaba Nedaei[a], Abtin Ataei[a], Muyiwa Samuel Adaramola[b], Alireza Hajiseyed Mirzahosseini[a], Morteza Khalaji Assadi[c] and Ehsanolah Assareh[d]

[a]Department of Energy Engineering, Graduate school of the Environment and Energy, Science and Research Branch, Islamic Azad University, Tehran, Iran; [b]Department of Ecology and Natural Resources Management, Faculty of Environmental Science and Technology, Norwegian University of Life Sciences, Ås, Norway; [c]Mechanical Engineering Department, Universiti Teknologi PETRONAS, Perak, Malaysia; [d]Department of Mechanical Engineering, Dezful Branch, Islamic Azad University, Dezful, Iran

**ABSTRACT**

Although there are many studies concerning the estimation of wind potential in different locations of Iran, an adequate evaluation of wind power for onshore locations of this country has not been investigated yet. The purpose of this research is to evaluate the potential of onshore wind in the south of Iran along the Gulf of Oman by comparing three Weibull numerical methods. In the first step, it became clear that the maximum likelihood method (MLM) compared to other methods represented the actual wind data with the lowest error rate and therefore it was selected as an accurate statistical distribution to model the wind speed of the investigated location. Using the MLM, the estimation of wind speed characteristics as well as the techno-economic evaluation of different wind turbines has been investigated. It was concluded that both technically and economically the studied area does not have sufficient wind power for the development of large-scale or grid-connected wind turbines. However, it may have enough power for non-grid-connected mechanical applications, such as wind generators for water pumping. Therefore, in the last part of this paper, an investigation of water pumping potential of the studied site by using adequate and modern wind turbines with lower start-up wind speed was recommended for future studies. Furthermore, it was suggested that the current methodology used in this research could be employed and extended in future studies to evaluate the wind potential of all onshore locations of Iran including onshore locations along the Persian Gulf and Caspian Sea.

**ARTICLE HISTORY**
Received 27 June 2015
Accepted 8 September 2016

**KEYWORDS**
Wind energy; wind turbine; Gulf of Oman; onshore wind; feasibility study

## 1. Introduction

Population growth and technological developments require the consumption of primary fossil fuel resources at a very fast pace, and hence shifting to alternative energy resources is an inevitable undertaking especially for importing countries. Therefore, environment-friendly renewable energy resources such as solar, hydro, wind, tidal energy, biomass and geothermal energy resources have attracted increasing investment worldwide in recent years. As many developed and developing countries are currently struggling to meet energy demands, devising programmes to bypass challenges in the use and deployment of such renewable energy resources has constituted an inter/national priority (Ataei et al. 2015a).

As one of the most economical sources of renewable energy resources, wind has a similar/lower production cost compared to that of fossil-based electricity production industries when considering greenhouse gas emissions. Not only is this energy resource found in abundance in most geographical locations, but it is also considered a profiting industry for landowners whose properties meet global wind resource standards while serving other economical purposes at the same time. Likewise, the availability of different types of multi-capacity wind turbine generators supports many small- or large-scale applications. For instance, at the former level, wind turbines can power remote locations without access to an electricity grid (Alamdari, Nematollahi, and Mirhosseini 2012; Nojedehi et al. 2016).

The earliest use of wind energy used for electricity production in the US dates back to the nineteenth century's windmills. Nowadays, using the wind energy for electricity production is a common trend as it is one of the most economical and environment-friendly renewable energy sources, avoiding $CO_2$ emissions and detrimental effects of greenhouse gases and climate change (Kose, Aksoy, and Ozgoren 2014). Based on the preliminary information provided by the World Wind Energy Association (WWEA), more than 50 GW of capacity was added during the year 2014, providing a total wind power capacity of close to 370 GW. The capacity for recently installed wind turbines was 40% more than in 2013, and substantially more than in the previous year (2012), when 44.6 GW were installed (WWEA 2015a). Moreover, a 2015 report (WWEA 2015b) showed that 105 countries in the world on all continents, including Antarctica, are using wind energy for electricity generation. In general, for the year 2030, WWEA sees a wind capacity close to two million MW as possible. Unfortunately, Iran's position in each year dropped

**CONTACT** Mojtaba Nedaei nedaei.mojtaba@gmail.com, mojtaba@khu.ac.kr; Muyiwa Samuel Adaramola (co-corresponding author) muyiwa.adaramola@nmbu.no

as follows: 43rd in 2011, 47th in 2012, 51st in 2013 and 54th in 2014 (WWEA 2015b). It is evident that Iran's use of wind energy is limited despite her abundant wind resources. Although several Iranian companies attempt to establish national power plants, more attention needs to be devoted to this sector.

### 1.1. Wind resource assessment review

The wind characteristics such as speed, direction and wind power are the major key parameters to determine the primary evaluation of wind power through a wind farm, for an investigated area. On this account, precise assessment of wind potential along with economic evaluation plays a significant role in wind energy utilisation for any location. Scanning the literature indicates extensive research and feasibility studies on wind power development around the world. For instance, wind resource assessment (WRA) has been done in China (Wua, Wanga, and Chib 2013) to address the potential of wind. It was found that the Logistic function provides a more adequate result compared to other distribution functions. According to a study of wind energy in Ghana (Adaramola, Agelin-Chaab, and Paul 2014), it was found that the wind resource in this area is suitable for large-scale wind energy development, small-scale applications and hybrid energy systems. Another study of WRA in Sindh, Pakistan, was done and it was concluded that the candidate site is recommended for some small stand-alone systems as well as for a wind farm (Khahro et al. 2013). The wind energy potential of Peninsular Malaysia was also investigated. It became clear that due to weak wind regimes, small-scale wind energy systems would be economically viable in a few regions most especially when the recently launched feed-in tariff in the country is extended to wind energy (Akorede et al. 2013). Using Weibull distribution, wind characteristics of four locations situated in Algerian Sahara were investigated by Boudia et al. (2013). In this study, Weibull coefficients were estimated and compared with the variation of air temperature for the studied locations. The obtained results indicated that wind speed is more uniform in the hottest periods. This led to conclude a possible correlation between air temperature and wind speed in the studied desert regions. Additionally it was also concluded that the highest energy output obtained from wind turbine with a capacity of 600 kW (Fuhrländer FL600) is found at the 'Bordj Badji Mokhtar' site, followed by 'Illizi', 'Djanet' and 'Tamanrasset'. Another analysis that was done for WRA of Dublin in Ireland by Sunderland, Mills, and Conlon (2013) showed that in conjunction with urban surface roughness, the urban frictional velocity must also be considered for urban wind resource modelling. Alamdari, Nematollahi, and Mirhosseini (2012) used the wind speed data for 68 studied areas during one year at different heights in Iran using Weibull distribution. GIS (Geographic Information System) themes for wind potential were also utilised in this research. In fact, GIS maps for average wind speed and power density of measurement data at three heights in Iran were presented. According to the maps, it was concluded that the eastern and north-western regions of Iran have good potential for development of wind turbines. These regions were situated in the path of strong wind flows. The central and southern regions of Iran do not have a relevant potential. Figure 1 demonstrates the map of GIS for average wind speed at 40 m height that was plotted for the whole of Iran in the aforementioned research.

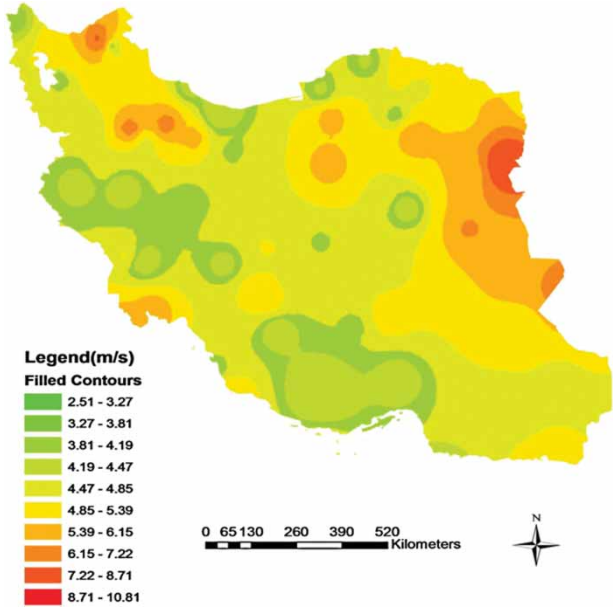


**Figure 1.** Map of GIS for average wind speed at 40 m in 68 sites in Iran.

### 1.2. Description of the investigated area

For the purpose of evaluating the potential of onshore wind, a meteorological mast was installed in an onshore location along the Gulf of Oman with geographical characteristics of longitude: 25° 41′ 7.7274″ and latitude: 58° 6′ 34.488″. This mast has recorded the wind data for the studied site during one year from 2012 to 2013 (SUNA 2015). The position of the studied region is demonstrated in Figure 2 (Google Earth 2015).

## 2. Material and methods

### 2.1. The proposed WRA tool

In this study, for the purpose of analysing the wind data and performing an adequate WRA, the Windographer™ modelling tool is utilised. The Windographer™ was first introduced and developed by Mistaya Engineering in 2006 but is now owned by AWS TruePower.

Figure 3 demonstrates the proposed flowchart of WRA framework using Windographer™, which is proposed in this study. In the first part, the raw wind data are extracted from the meteorological mast and then these data are imported to the Windographer™. In the 'Visualising' part, a wide range of options can be provided to allow us to explore and understand the wind data in a clear way. In the next step, we can configure the wind data or change them by applying scaling factors, shifting some or all of the data in time, deleting segments of data, filling gaps, or extrapolating vertically (using power law or logarithmic law). Quality control is the filtering capability which can help us to find and filter out problem data segments. By running the analysis, we were able to explore the intricacies of wind shear, turbulence intensity, tower distortion, extreme winds, wind turbine output and more. In the last step, by taking into account the obtained results in the previous steps, a comprehensive evaluation of WRA for an investigated region can be accomplished (Windographer™ 2015).


**Figure 2.** Position of the studied onshore area along the Gulf of Oman.

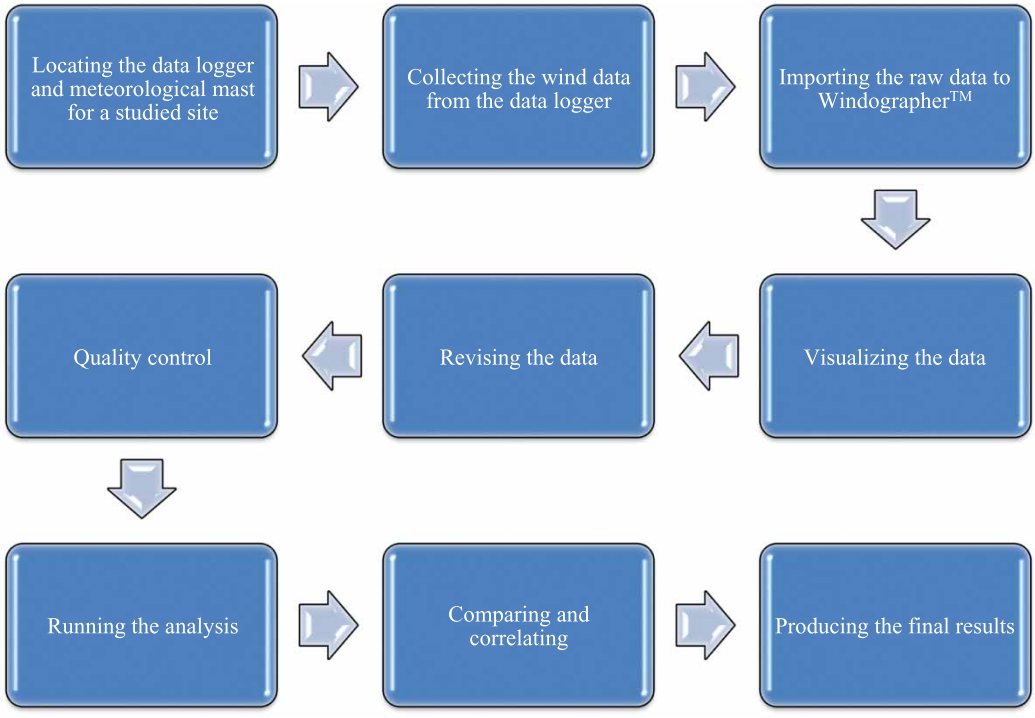


**Figure 3.** The proposed flowchart of WRA framework using Windographer™.

### 2.2. *Numerical methods for determining the Weibull parameters*

In order to perform a precise WRA for an investigated location, the statistical analysis is the best solution for predicting the distribution of wind speed. Common distribution functions for analysing the wind data are Weibull, Rayleigh, Log-normal and Logistic. The experimental research has demonstrated that the Weibull distribution is the best method for assessing the wind resource of a given region, with an acceptable accuracy level. The Weibull distribution function is named after Waloddi Weibull in 1951 and has widely been used for characterising wind regimes. The function can be described as a probability density function $f(U)$ and a cumulative distribution function $F(U)$, determined by the following equations (Biglari et al. 2013; Fazelpour et al. 2015):

$$f(U) = \frac{k}{c}\left(\frac{U}{c}\right)^{k-1} \exp\left[-\left(\frac{U}{c}\right)^{k}\right], \quad (1)$$

$$F(U) = 1 - \exp\left[-\left(\frac{U}{c}\right)^{k}\right]. \quad (2)$$

In the above equations, $U$ is the wind speed value, $c$ is the Weibull scale parameter and $k$ is the dimensionless Weibull shape parameter. In this study, three numerical methods are used to determine and estimate the Weibull parameters $c$ and $k$:

(1) Maximum likelihood method (MLM)
(2) Least squares algorithm (LSA) (graphical method)

(3) Method of moments (MM) (WAsP international model also uses the method of moment for Weibull fitting)

In the following, a brief description of each method has been addressed. Then in Section 3, a comparison of each method has been presented.

#### 2.2.1. Maximum likelihood method

According to Seguro (Seguro and Lambert 2000), the MLM is suggested for utilisation with time series wind data. The maximum likelihood estimation method is a relatively complicated method since it requires extensive numerical iterations for determining the Weibull parameters. This method employs the following equation to calculate the Weibull $k$ parameter in an iterative method (Seguro and Lambert 2000):

$$k = \left[ \frac{\sum_{i=1}^{N} U_i^k \ln(U_i)}{\sum_{i=1}^{N} U_i^k} - \frac{\sum_{i=1}^{N} \ln(U_i)}{N} \right]^{-1}, \tag{3}$$

where $U_i$ is the wind speed in time step $i$ and $N$ is the number of time steps. Once the shape parameter $k$ has been found, the following equation estimates the value of the scale parameter $c$:

$$c = \left( \frac{\sum_{i=1}^{N} U_i^k}{N} \right)^{1/k}. \tag{4}$$

#### 2.2.2. Least squares algorithm

The LSA or graphical method can be obtained by a double logarithmic transformation of the cumulative distribution function. In this distribution method, the wind speed data are interpolated by a straight line, using the concept of least squares. The following equation represents the graphical method (Costa Rocha et al. 2012):

$$\ln\left\{\ln\left[\frac{1}{(1-F(U))}\right]\right\} = k \times \ln(U) - k \times \ln(c). \tag{5}$$

The above equation is in the general slope-intercept form: $y = mx + b$. So, if we were to plot ln ($U$) on the $x$-axis and ln {ln[1/(1−$F(U)$)]} on the $y$-axis, we would expect a straight line with slope equal to $k$ and intercept equal to $-k \times$ ln ($c$).

Accordingly, to determine the best-fit Weibull distribution based on the LSA, ln ($U$) and ln {ln[1/(1−$F(U)$)]} are estimated for every data point; afterwards those values are put into a linear least squares solver to determine the slope and intercept of the line of best fit. At last, $k$ is set equal to the slope of that line, and $c$ equal to exp (−intercept/slope).

#### 2.2.3. Method of moments

MM is one of the methods employed for calculating the values of $c$ and $k$, which is based on numerical iteration. This method is also suggested as an alternative for the MLM. By employing this algorithm, the Weibull $k$ parameter can be calculated by Equation (5) (Chang 2011):

$$\sigma = c\left[\Gamma\left(1+\frac{2}{k}\right) - \Gamma^2\left(1+\frac{1}{k}\right)\right]^{1/2}. \tag{6}$$

Once the shape parameter $k$ is estimated, the following equation gives the value of the scale parameter $c$:

$$c = \frac{\bar{U}}{\Gamma\left(1+\frac{1}{k}\right)}, \tag{7}$$

where $U$ is the wind speed value and $\bar{U}$ is the average wind speed, which can be calculated according to Equation (7):

$$\bar{U} = \frac{1}{n}\sum_{i=1}^{n} U_i. \tag{8}$$

The variance, $\sigma^2$, of wind velocity recordings is:

$$\sigma^2 = \frac{1}{n-1}\sum_{i=1}^{n} (U_i - \bar{U})^2. \tag{9}$$

Average wind speed and the variance of wind velocity could be estimated based on the values of the Weibull parameters as described below:

$$\bar{U} = c\Gamma\left(1+\frac{1}{k}\right), \tag{10}$$

$$\sigma^2 = c^2\left[\Gamma\left(1+\frac{2}{k}\right) - \Gamma^2\left(1+\frac{1}{k}\right)\right]. \tag{11}$$

And the gamma function of ($x$) (standard formula) can be estimated as follows:

$$\Gamma(x) = \int_0^{\infty} e^{-u} u^{x-1} du. \tag{12}$$

### 2.3. Evaluation of the investigated methods for calculating the Weibull coefficients

For the purpose of assessing the performance of the investigated distributions, the mean root-square error (RMSE) parameter as well as the $R$ Squared ($R^2$) were employed (Windographer™ 2015).

The RMSE parameter provides the deviation between the forecasted and the theoretical values; it must be as close to zero as possible, and it is estimated according to the following equation:

$$\text{RMSE} = \sqrt{\frac{\sum_{i=1}^{N} (y_i - x_i)^2}{N}}, \tag{13}$$

where $y_i$ are the actual values of $y$, and $x_i$ are the values computed from the correlation equation for the same value of $x$. The smaller the values of RMSE are, the better the curve fits. Basically, RMSE should approach zero values.

$R^2$ shows the performance of a studied model and is used to describe how well a regression line fits a set of data. $R^2$ is observed as a number between 0 and 1.0. An $R^2$ close to 1.0 implies that a regression line fits the data very well. So, in this study, $R^2$ is employed as a goodness of fit parameter, which shows how closely the fitted Weibull distribution matches the

frequency histogram of the actual data. $R^2$ can be estimated as:

$$R^2 = \frac{\sum_{i=1}^{N}(y_i - z^*)^2 - \sum_{i=1}^{N}(x_i - y_i)^2}{\sum_{i=1}^{N}(y_i - z^*)^2}, \quad (14)$$

where $y_i$ is the $i$th experimental data, $z^*$ is the mean value of the experimental data, $x_i$ is the $i$th predicted data with the Weibull distribution and $N$ is the number of observations.

### 2.4. Modelling tool for analysis of the studied methods

For the purpose of applying the three aforementioned models (MLM, LSA and MM) to the wind data of the investigated region, the wind distribution analysis module of Windographer™ software was employed. This module uses Equations (1)–(14) to analyse the wind data by using the three mentioned models. As an example for the MLM algorithm, by having the mean wind speed in time step $i$ ($U_i$) and the number of time steps ($N$), Equations (3) and (4) are used to estimate the $k$ and $c$ values of the Weibull function. Accordingly, these values for the two other models, that is, LSA and MM, can be estimated based on the next equations. In addition to the $k$ and $c$ values calculated for each method, Equations (13) and (14) are used to calculate the RMSE and $R^2$ (the goodness-of-fit parameters) to indicate how closely the fitted Weibull distribution matches the frequency histogram of the measured wind data, making it possible to quickly determine the best method with the highest accuracy.

### 2.5. Wind power density

The power of the wind that flows at speed $U$ through a blade sweep area $A$ increases with the cube of the wind speed and the area, which is (Nedaei et al. 2016):

$$\frac{P}{A} = \frac{1}{2}\rho U^3, \quad (15)$$

where $\rho$ is the air density. Wind power density (WPD), expressed in Watt per square metre (W/m$^2$), considers the frequency distribution of the wind speed and the reliance of wind power on air density and the cube of the wind speed. Thus, WPD is usually assumed as a better indicator of the wind energy resource than wind speed values alone. The mean WPD can be estimated using the following equation (Nedaei 2014):

$$\left(\frac{P}{A}\right)_{\text{avg}} = \frac{1}{2n}\sum_{i=1}^{n}\rho(U_i^3). \quad (16)$$

In the above equation, $U_i$ is the calculated wind speed in the time interval of 10 min and $N$ is the total sample data used for each year (Keyhani et al. 2010).

Additionally, estimation of the WPD based on the Weibull distribution function can be fulfilled according to the following equation (Keyhani et al. 2010):

$$\left(\frac{P}{A}\right)_{\text{Weibull}} = \int_0^{\infty}\frac{1}{2}\rho U^3 f(U)\mathrm{d}U = \frac{1}{2}\rho c^3\Gamma\left(\frac{k+3}{k}\right). \quad (17)$$

### 2.6. Turbulence intensity

Wind turbulence intensity – which is the set of random and continuously changing air motions – is considered as one of the primary features of a wind farm. Wind turbulence can have a negative effect on the power performance of a wind turbine; it can also cause extreme loading on the wind turbine components. According to Equation (24), the wind turbulence intensity can be defined as the ratio of standard deviation $\sigma$ to the mean wind speed $U$ (Ahmed 2011):

$$\text{TI} = \frac{\sigma}{U}, \quad (18)$$

where $\sigma$ is the standard deviation of wind speed within each time step, $U$ is the mean wind speed and TI is the turbulence intensity which is expressed as a fraction.

#### 2.6.1. Calculating the turbulence intensity for different direction sectors

In Figure 4, the annual average turbulence intensity at 40 m height is calculated for different direction sectors using the wind direction sensor of 37.5 m. It can be observed that the mean turbulence intensity values are more considerable for northwest and southeast direction sectors. As can be seen, the maximum values of mean turbulence intensity are shown for both northwest and southeast with a value of almost 0.18.

The next figure (Figure 5) shows the peak values of turbulence intensity at 40 m height (using the direction sensor of 37.5 m) for the studied site. As can be seen, the maximum peak values occurred in the direction sectors of 292.5° and 225° with a value of approximately 3.3.

### 2.7. Surface roughness

The surface roughness (sometimes called surface roughness length or just roughness length) is defined as an effective height above the surface where wind speed reduces to zero. It is a parameter in the logarithmic law, which states that the wind speed varies logarithmically with the height above ground

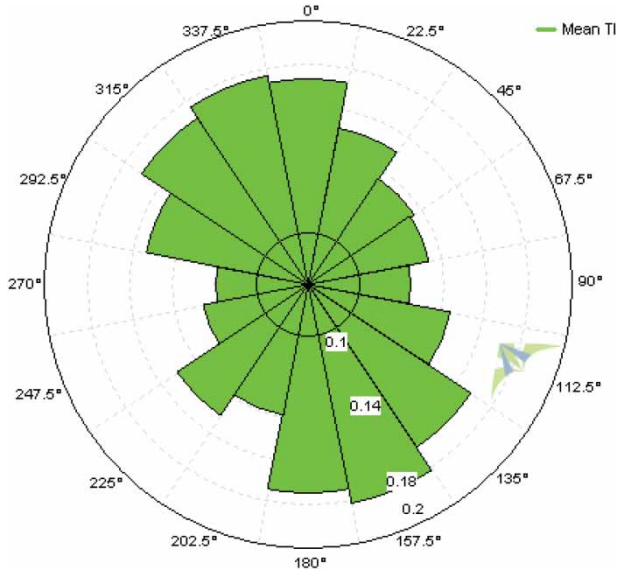


**Figure 4.** The annual average wind turbulence intensity for different direction sectors.

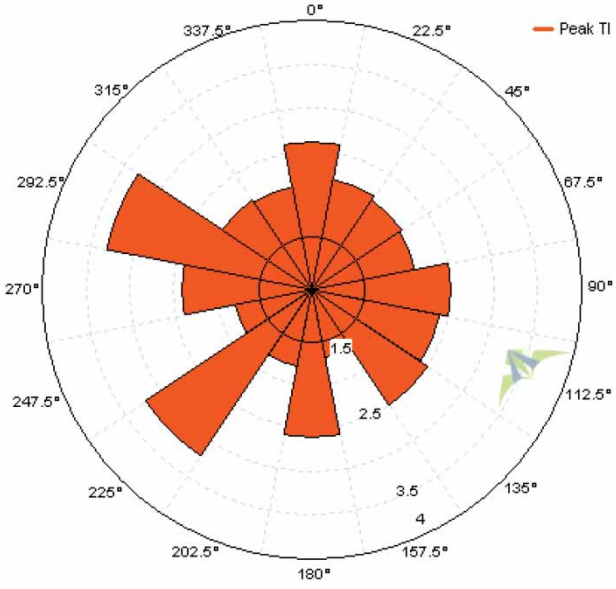


**Figure 5.** The peak values of wind turbulence intensity for different direction sectors.

according to the following equation (Gualtieri 2015):

$$U(z) = \begin{cases} \frac{U^*}{k}\ln\left(\frac{z}{z_0}\right), & \text{if } z < z_0 \\ 0, & \text{if } z < z_0 \end{cases}, \tag{19}$$

where $U(z)$ is the wind speed [m/s] at some height above ground $z$ [m], $U^*$ is the friction velocity [m/s], $k$ is von Karman's constant (0.4), $z_0$ is the surface roughness [m], ln is the natural logarithm.

### 2.7.1. Calculation procedure for the surface roughness

For data sets that contain wind speed data for two or more heights above ground, the surface roughness value that best fits the measured vertical wind speed profile can be obtained. We can use a linear LSA to fit the logarithmic profile to the measured wind speed data. Using the rule $\ln(1/x) = -\ln(x)$, we can rewrite the logarithmic law as follows (Jain 2010):

$$U(z) = \frac{U^*}{k}\ln(z) - \frac{U^*}{k}\ln(z_0). \tag{20}$$

This equation is now in the general slope-intercept form: $y = mx + b$. A plot of wind speed versus the logarithm of height would therefore produce a straight line with:

$$\text{Slope} = \frac{U^*}{k}. \tag{21}$$

The linear least squares regression can be employed to find the line of best fit for this function, and then the surface roughness can be estimated using the following equation:

$$z_0 = \exp\left(-\frac{\text{intercept}}{\text{Slope}}\right), \tag{22}$$

The graph in Figure 6 shows the effect of the surface roughness on the wind shear profile of the studied site predicted by the logarithmic law. It is worthy to note that wind shear demonstrates the rate at which wind speed changes with height. It is generally influenced by the surface roughness.

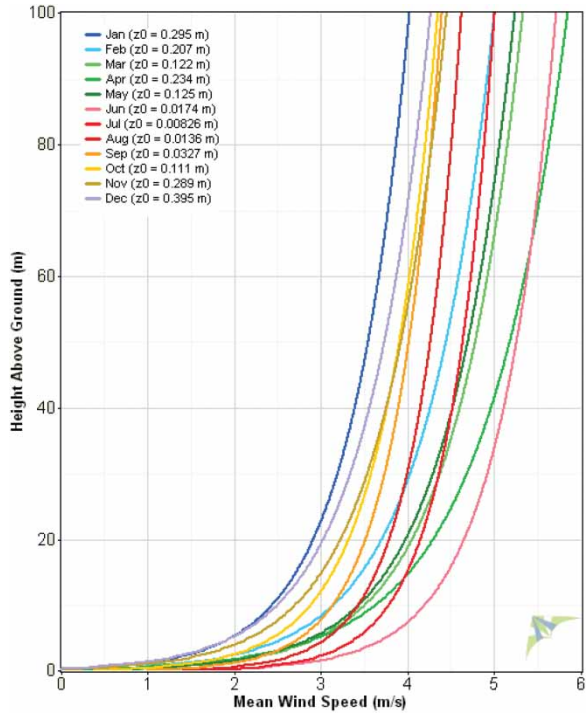


**Figure 6.** The effect of the surface roughness on the wind shear profile of the studied site.

As can be seen in Figure 6, each line on the graph corresponds to a different value of surface roughness. Clearly surface roughness ($Z_0$) is ranged from a minimum of 0.00777 m in July to a maximum of 0.361 m in December. It can also be realised that, for example, at a height of 50 m, the lowest mean wind speed occurred in Jan with a value of 3.5 m/s, while the highest mean wind speed occurred in Jun with a value of 5.25 m/s.

### 2.7.2. Estimating the roughness of the ground at different directions

The surface roughness of the ground based on the wind speed and direction is demonstrated in Figure 7. The calculations are made on the basis of the wind data from the direction sensor of 37.5 m and wind speed sensor of 40 m. According to Figure 7, it can be concluded that there seem to be more ground obstacles from the west and northwest (from the direction sector of 270° to 330°) because of the higher values of surface roughness in these sectors, while the lower values of surface roughness are observed for the east and northeast (from the direction sector of 60° to 90°). It is clear that in the west of the mast location, the amount of the surface roughness can reach its maximum value (1.20 m), while other direction sectors did not experience significant values of surface roughness. Maximum surface roughness values are observed in the west direction from 270° to 330°. The violet colour in the graph indicates the minimum values of surface roughness ranging from 0 to 0.12 m. Another issue that can be inferred from Figure 7 is the demonstration of wind speed scales with respect to the surface roughness values in different directions. In fact is, this shows the relation between wind speed values at 40 m height as well as surface roughness of the studied site at different direction sectors. By way of an example, as can be seen in Figure 7, in the direction sector of 150°, when the surface

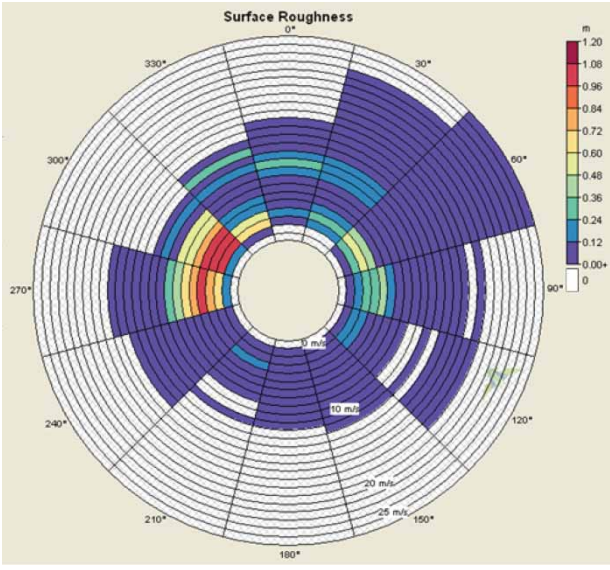


**Figure 7.** The surface roughness of the ground based on the direction.

roughness ranges from 0 to 0.12 m, the wind speed values range from 0 to 11 m/s.

#### 2.7.3. Estimating the wind speed at different heights

In the field of WRA, two common methods, power law as well as logarithmic law, are widely used for the purpose of wind speed prediction at higher elevations. Experimental research has demonstrated that, in the low parts of the planetary boundary layer, for example, heights lower than 20 m, the logarithmic method seems to provide more accurate results. As height goes up from 20 to 100 m, both methods would become reliable. On the other hand, from 100 m to near the top of the atmospheric boundary layer the power law produces more precise predictions of mean wind speed (Assareh et al., forthcoming; Cook 1986).

In this study, for the purpose of calculating the wind speed values at a 15 m height, the log law method is utilised. This method employs the procedure described in Equations (19)–(22) in order to estimate the wind speed at higher heights. The results of the predictions are shown in Section 3.4.

### 2.8. Wind turbine energy production

If we consider $f(U)$ as wind speed probability distribution function, and $P_w(U)$ as the wind turbine power curve, it is possible to calculate the average wind turbine power ($P_W$) as follows (Mirhosseini, Sharifi, and Sedaghat 2011):

$$P_W = \int_0^\infty P_w(U) f(U) \mathrm{d}U. \tag{23}$$

So, with a summation over $N_B$ (total sample data used for each year), the following equation can be used to estimate the average wind turbine power:

$$P_W = \sum_{i=1}^{N_B} \frac{1}{2}(U_{i+1} - U_i)(f(U_{i+1})P_w(U_{i+1}) + f(U_i)P_w(U_i)). \tag{24}$$

Therefore, by using the above equation for the average wind turbine power, the annual wind power harnessed from the turbine can be estimated as follows:

$$E_W = P_W \times N \times \Delta t, \tag{25}$$

where $N$ is the number of measurement periods ($\Delta t$).

### 2.9. Economic analysis

If we consider $C_I$ as the preliminary capital cost of the wind turbine and $C_{OM}$ as the operation and maintenance cost including salary, insurance, tax, rent and salvage value, the $C_{OM}$ can be described as a percentage (m) of $C_I$ (Mostafaeipour et al. 2011):

$$C_{OM} = mC_I. \tag{26}$$

By considering $P_R$ as the potential (theoretical) energy output of the turbine, and CF as the capacity factor, we can then calculate the actual energy output ($E_I$) of the turbine in a year as follows:

$$E_I = 8760 \times P_R \times \mathrm{CF}. \tag{27}$$

Capacity factor (CF), which is a dimensionless quantity, is defined as an indicator of the generated electricity per kW of installed capacity (kWh/kW) per year. It mainly depends on the wind speed distribution and the design of the wind turbine. Using the CF, the unit cost of electricity can be estimated as follows (Kandpal and Grag 2003):

$$\mathrm{UCE} = \frac{C_I(\mathrm{CRF} + m)}{8760(P_R)(\mathrm{CF})}. \tag{28}$$

In the above equation, CRF is the capital recovery factor and can be described as (Abam and Ohunakin 2015):

$$\mathrm{CRF} = \frac{d(1+d)^t}{(1+d)^t - 1}, \tag{29}$$

where $d$ is the annual interest rate and $t$ is the useful life of the system (Ataei et al. 2015b).

## 3. Results and discussion

Wind data were extracted from a data logger located in the studied site and have been statistically analysed to evaluate the potential of the onshore wind in the investigated area. The data logger used has three sensors of velocity at 10, 30 and 40 m heights and also two sensors of direction at 30 and 37.5 m. The wind sensor type is 'P2546A-OPR' designed by a Danish company (WINDSENSOR 2015). Wind data were measured with the time interval of 10 min from 1.07.2007 to 25.07.2008 by a data logger type 'METEO-40S' manufactured by a German company (Ammonit Measurement GmbH 2015). The logging interval – which is the period of time over which measurements are taken by the sensors – is considered to be 10 min. In addition, the installed mounting structure and wind mast type is WMI Type 3, which is ideal for long-term WRA for a specific site (WMI 2015). The solidity rate for this mast is estimated to be 0.25. Furthermore, we sampled the wind data at 1 Hz, one sample every second. Table 1 briefly describes the information concerning wind mast and wind sensor characteristics.

**Table 1.** Wind mast and wind sensor characteristics.

| Characteristics | Value/model (type) |
|---|---|
| Wind data recovery rate | 96% |
| Wind data sampling rate | 1 Hz |
| Wind mast type | WMI Type 3 |
| Wind sensor type (cup anemometer) | P2546A-OPR |
| Wind vane | Theodor Friedrichs & CO (2016) |
| Wind data logger model | METEO-40S – Ammonit |
| Logging interval of data logger | 10 min |
| Number of all recorded data points | 1,102,320 |

It can be seen in Table 1 that the percentage of wind data recovery rate for three heights of 10, 30 and 40 m is 96%. The following equation is used to calculate the data recovery rate:

$$\text{Data recovery rate} = \frac{N_{\text{valid}}}{N_{\text{possible}}}.100\%, \tag{30}$$

where $N_{\text{valid}}$ is the number of valid data points in the time interval (invalid data points are those missing wind data); $N_{\text{possible}}$ is the possible number of data points in the time interval.

In this study among all 1,102,320 data points, 881,856 data points are related to the wind data (wind speed and direction at different heights) and the rest of the data points are for humidity, solar radiation, temperature and air density.

### 3.1. Wind speed distribution of the onshore investigated area

By employing the three numerical methods, that is, maximum likelihood, least squares and WAsP (MM), the graphical result for Weibull distribution of wind speed is presented in Figures 8–10 for three heights of 10, 30 and 40 m. The graphical results show that by increasing the height, there would be more compatibility between the actual wind data and the three investigated numerical methods. It is clear that these three methods have relatively suitable compatibility with the actual wind data. However, for precise evaluation of these three numerical methods, it is necessary to compare each of them by performing an error analysis.

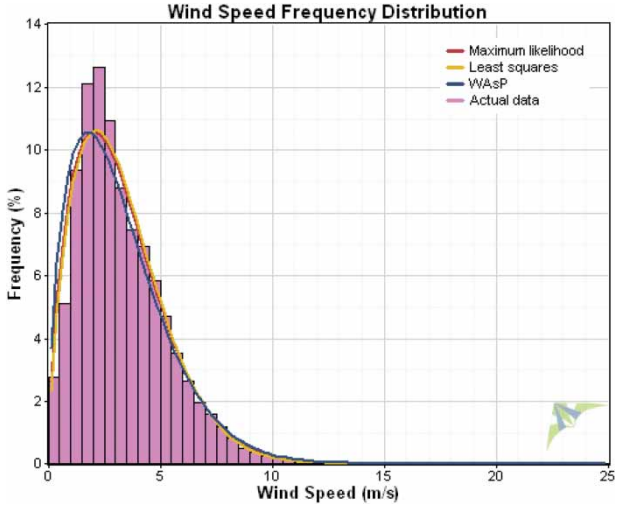


**Figure 8.** Wind speed distribution for the studied site using three numerical methods at 10 m.

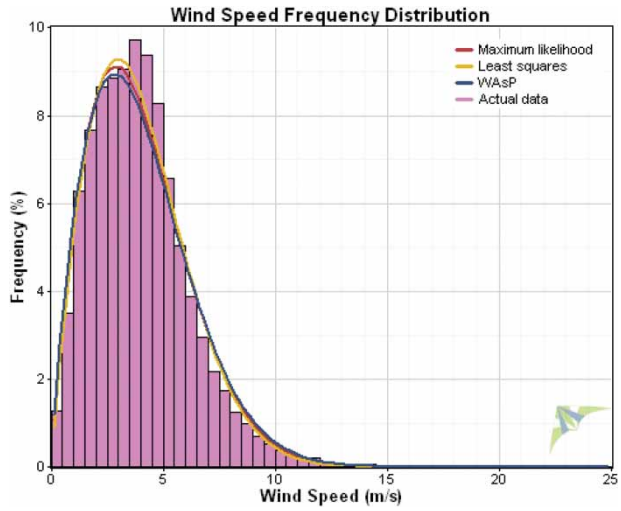


**Figure 9.** Wind speed distribution for the studied site using three numerical methods at 30 m.

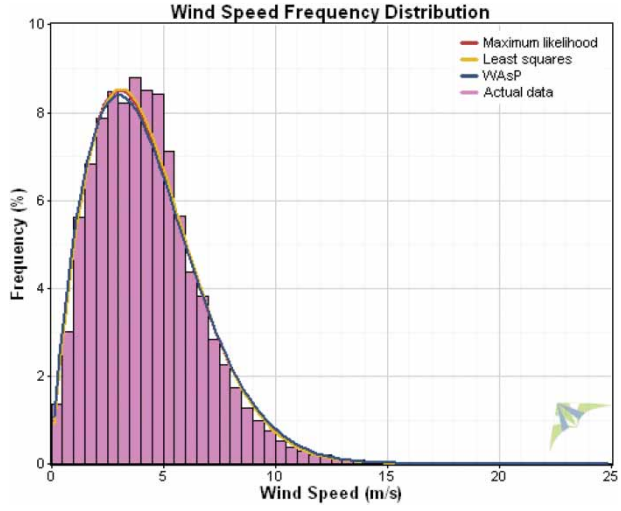


**Figure 10.** Wind speed distribution for the studied site using three numerical methods at 40 m.

**Table 2.** Performance evaluation of three numerical methods for obtaining Weibull parameters in the investigated area at three heights of 10, 30 and 40 m.

| Algorithm | Height (m) | Weibull $k$ | Weibull $c$ (m/s) | $R^2$ | RMSE |
|---|---|---|---|---|---|
| MLM | – | | | | |
| | 10 | 1.639 | 3.632 | 0.9788 | 0.0091 |
| | 30 | 1.826 | 4.451 | 0.9906 | 0.0058 |
| | 40 | 1.639 | 4.753 | 0.9919 | 0.0043 |
| Least squares | – | | | | |
| | 10 | 1.680 | 3.658 | 0.9772 | 0.0101 |
| | 30 | 1.886 | 4.457 | 0.9876 | 0.0083 |
| | 40 | 1.843 | 4.489 | 0.9907 | 0.0056 |
| WAsP | – | | | | |
| | 10 | 1.526 | 3.546 | 0.9625 | 0.0122 |
| | 30 | 1.791 | 4.489 | 0.9840 | 0.0089 |
| | 40 | 1.787 | 4.781 | 0.9881 | 0.0073 |

In Table 2, performance evaluation of the three aforementioned numerical methods, for obtaining the Weibull coefficients ($c$ and $k$) in the investigated area, has been performed. For this purpose, two error evaluators, that is, $R^2$ as well as RMSE, are utilised to assess the performance of the three studied models. According to these evaluators, a method better approximates

the actual data when the values of RMSE are close to zero, and the values of $R^2$ approach unity. By inspecting the tabular results, it can be concluded that even though the difference between the aforementioned methods is relatively small, in all cases, the MLM as well as the graphical method (least squares) appeared to represent the actual data better. As can be seen in Table 2, Weibull coefficients with the lowest error rate ($R^2 > 0.9900$ and RMSE $< 0.0060$) have been highlighted with yellow colour. Generally, it has been demonstrated that in the investigated area, at all three heights, MLM in comparison with other methods gives the highest values of $R^2$ and the lowest values of RMSE. Therefore, in the next parts of this study, the MLM was selected as the accurate statistical distribution to model the wind speed of the studied location.

One of the interesting findings of this research is that by inspecting the graphical and tabular results (Figures 8–10 and Table 2) it can be realised that by increasing the height, three mentioned models would have a better compatibility with the actual wind data, while at lower heights the errors become more significant. According to a new research published by Elsevier (Nedaei, Assareh, and Biglari 2014) it has been demonstrated that the turbulence intensity of the wind (TI) as well as the roughness of the ground (surface roughness) can effectively influence the compatibility of the wind data with Weibull distribution function. These two key parameters (TI and the surface roughness) for the studied site were estimated by using the methodology described in Sections 2.5 and 2.6. According to the graphical evaluation of TI provided in Figures 11–13 for three heights of 10, 30 and 40 m, the maximum values of turbulence intensity estimated for each height varies from 4.70 at 30 m height (Figure 12) and 3.80 at 10 m height (Figure 11) to 3.30 at 40 m height (Figure 13). In addition, the average maximum values of the turbulence intensity are estimated as 0.2 for 10 m height, 0.16 for 30 m height and 0.14 for 40 m height. Therefore, it is evident that height above ground level in the studied area has less effect on the value of wind turbulence intensity. Additionally, it can be realised that the TI values at 10, 30 and 40 m heights are not very considerable.

On the other hand, the surface roughness of the studied location was estimated to be 0.08 m. Accordingly, the roughness class obtained was 1.91. Nedaei, Assareh, and Biglari (2014) developed a classification of terrain characterised by roughness class. According to this classification, it can be realised that our investigated location is characterised as an agricultural land with some houses and at least 8-m tall sheltering hedgerows. According to meteorological information obtained from SUNA organisation database (SUNA 2015), the current analytical results for surface roughness in the studied site are also compatible with the observed in-situ surface roughness.

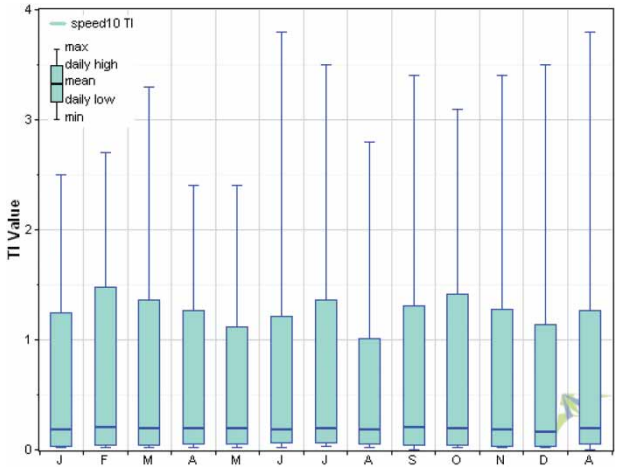


**Figure 11.** Monthly analysis of TI for the investigated area at 10 m height.

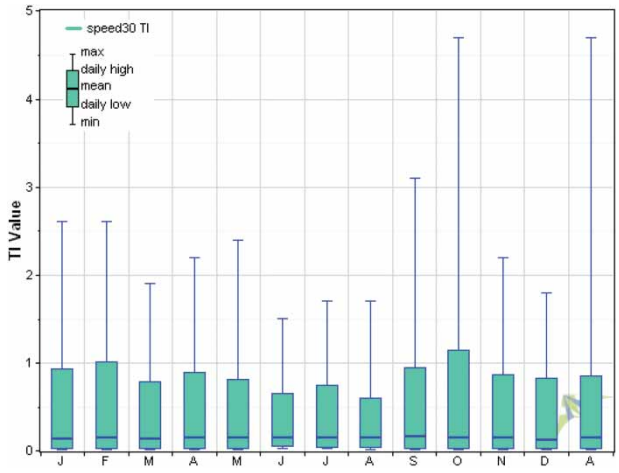


**Figure 12.** Monthly analysis of TI for the investigated area at 30 m height.

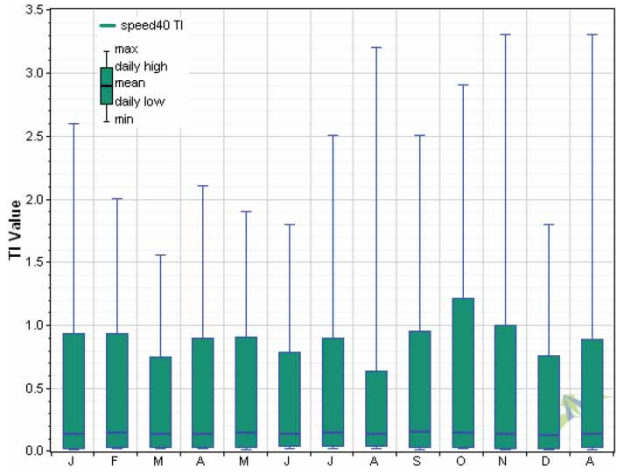


**Figure 13.** Monthly analysis of TI for the investigated area at 40 m height.

### 3.2. Wind speed characteristics

As it was explained in the previous section (Section 3.1), the MLM was found to be the best algorithm in the studied site for modelling the wind speed characteristics. So, by using this method, in this section, an analysis of monthly as well as diurnal wind speed profile, cumulative distribution of wind speed, wind direction and WPD has been performed.

Monthly average wind speed profile for the investigated area at different heights is demonstrated in Figure 14. As it can be seen, at 40 m height, for seven months of the year, from February to August, the mean wind speed is more than 4 m/s. Out of these seven months, two months (April and June) have the average wind speed of more than 5 m/s. So, these two months

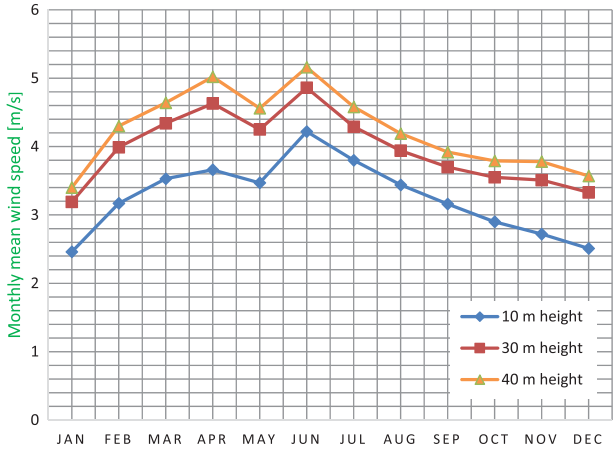


**Figure 14.** Monthly average wind speed profile in the investigated area.

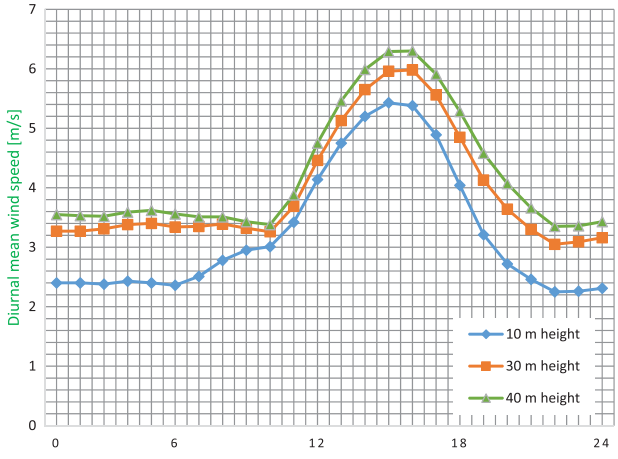


**Figure 15.** Diurnal wind speed profile in the investigated area.

are more suitable for wind power production compared to other months of the year. The maximum mean wind speed occurred in June with a value of 5.20 m/s. In the months of January, September, October, November and December the mean wind speed ranged from 3.38 m/s (minimum wind speed all over the year) in January to 3.95 m/s in September. Therefore, these months are not suitable for harnessing the wind power. The average wind speed for the whole of the year in the studied site is estimated to be 4.3 m/s.

Additionally, diurnal wind speed profile is demonstrated in Figure 15. This figure shows hours of day with suitable wind speed all over the year. As it can be observed, in the studied site, best wind speed values happen during the afternoon (almost from 12 pm to 6 pm).

The wind direction plays an important role in the optimum positioning of a wind farm in an investigated region. In this study, monthly and hourly wind direction diagrams are presented in Figures 16 and 17. As can be seen in Figure 16, the prevailing wind direction in the months of February, March, April and May is mostly from the west, while the dominant wind direction for the months of June, July and August is mostly from the southeast. In fact, one of the findings of this research is that according to Figure 16, in different months of the year, there are a wide variety of dominant wind directions. For example in January, the prevailing wind direction is from northeast, while the dominant wind direction in February is from the west. This shows that apparently in the studied onshore location in the south of Iran, the prevailing wind direction is always changing. Additionally Figure 17 demonstrates that from 12 am to 10 am, the direction of the wind is mostly from the east. At 8 am the prevailing wind direction starts to divert. Furthermore, from 12 pm to 8 pm, the dominant wind direction is mostly from the west. In addition to the monthly and hourly diagrams of wind direction for the studied site, the annual wind rose (Figure 18) is also presented which shows the average direction of the wind for 12 months at a 37.5-m height in the investigated area. According to this figure, it can be concluded that the predominant wind direction is mostly from both the west and the east (but in general it can be inferred that wind blows not just from the east and west but also from all directions).

Figure 19 illustrates the cumulative distribution of wind speed at three heights. It demonstrates the time fraction or probability that the wind speed is greater than or equal to a specified wind speed value. It can be understood that the wind speed at 10, 30 and 40 m heights is greater than 3.5 m/s for 38%, 55% and 58% of the time. The 3.5 m/s is an important limit since this is the cut-in speed of many small wind turbines.

Determining the average wind speed in a studied site is not the final step to evaluate the accessible wind potential in the proposed site. Accordingly, the WPD is a crucial parameter for providing the information about selecting an appropriate site and also estimating the immediate wind power classification of that site. For this main reason, the existing WPD in the studied site has been estimated. In Figure 20, the monthly wind power densities at three heights are determined by the measured data. The WPD at 40 m height ranged from a minimum of almost 45 W/m$^2$ in January (and December) to a maximum of 238.5 W/m$^2$ in the middle of June. Furthermore, WPD values of more than 200 W/m$^2$ at heights of 30 and 10 m have not been observed. Additionally the average wind power densities at heights of 10, 30 and 40 m are estimated to be 48, 79 and 101 W/m$^2$, respectively. According to the world classification of wind power described in Ahmed (2011), it became clear that the wind power class for the investigated onshore area is 1 which is considered 'poor'.

In order to determine the direction of wind with the highest net energy production, the WPD for wind speed sensor of 40 m is calculated for each time step. Then the values are sorted by the direction sensor of 37.5 m and finally the total net energy available for the noted direction sensor is estimated over the entire period of the wind data set. As a result, Figure 21 is outlined which demonstrates the portion of the total wind energy coming from each direction sector. The figure shows that about 23% of the total amount of energy in the wind comes from the west direction, with another 16% coming from the southwest direction (direction sector of 247.5°) and about 20% coming from two east sectors (from 67.5° to 90°).

### 3.3. The see breeze effect

In coastal regions, sea and land breezes can have a significant effect on wind speed and direction. According to Figure 22, the sea breeze is described as a breeze that blows from the sea

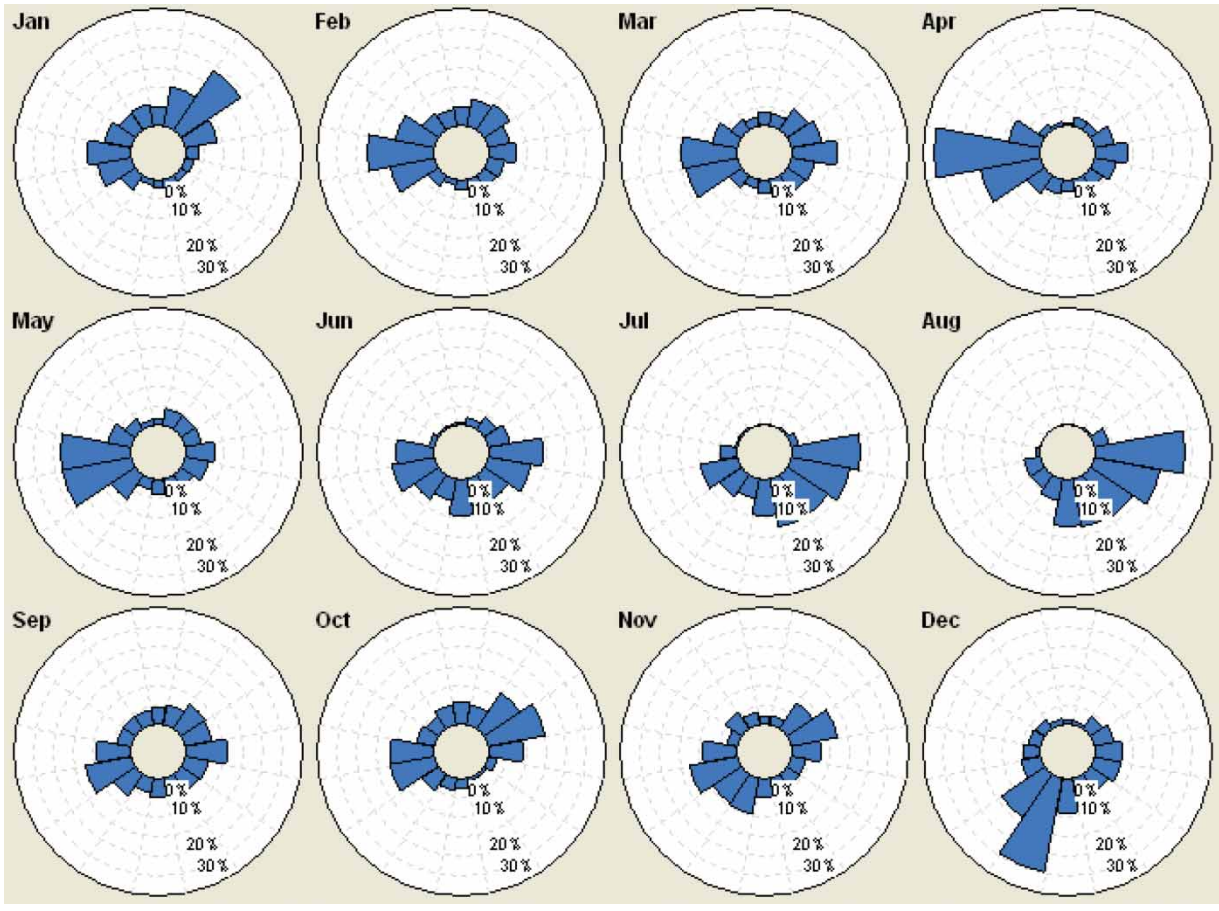


**Figure 16.** Monthly wind speed direction at 37.5 m.

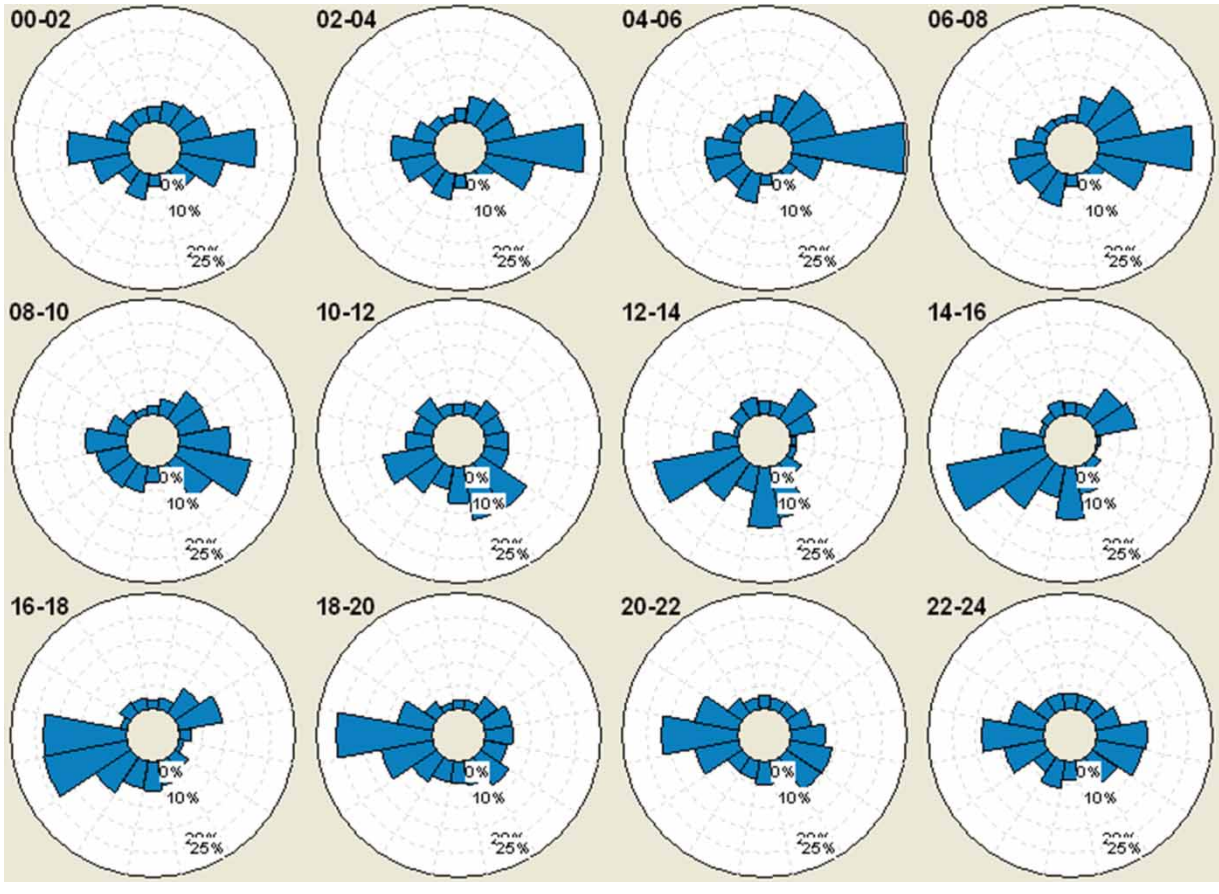


**Figure 17.** Hourly wind speed direction at 37.5 m.

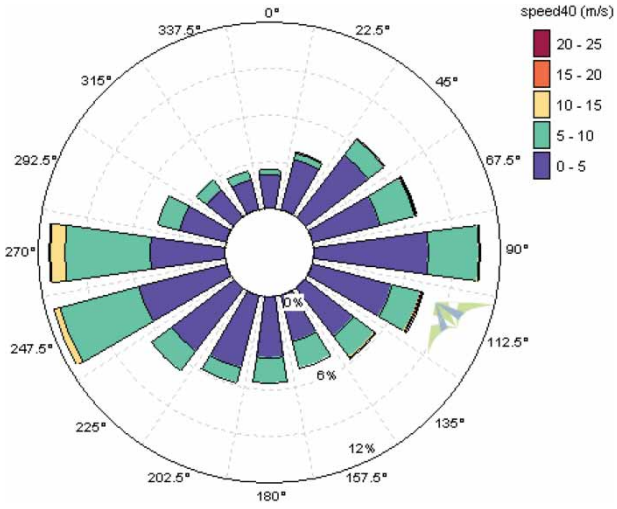


**Figure 18.** Annual wind direction in the studied site at a height of 37.5 m.

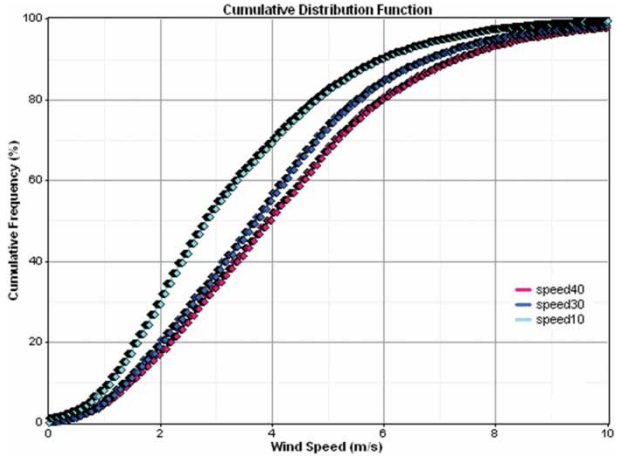


**Figure 19.** Cumulative distribution of wind speed in the studied area at different heights.

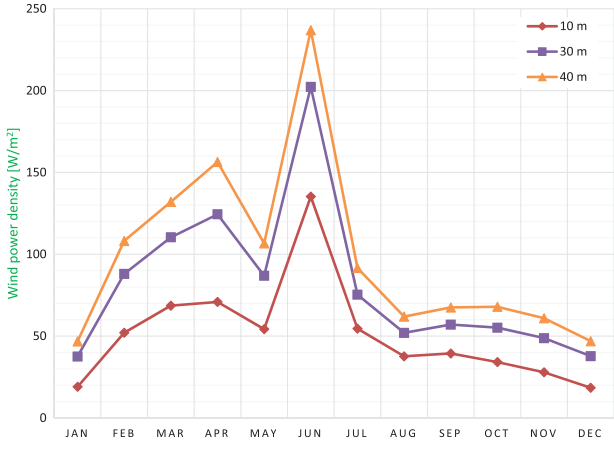


**Figure 20.** Monthly WPD at three heights.

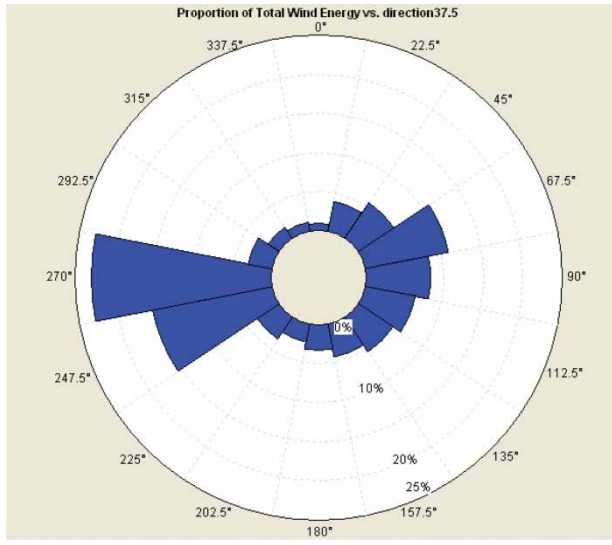


**Figure 21.** The Proportion of net wind power according to the direction sector.

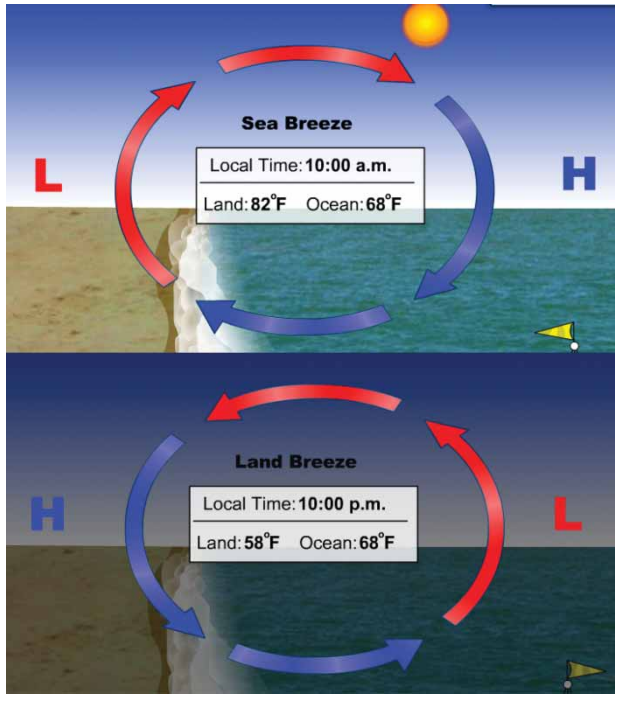


**Figure 22.** The sea and land breeze circulation.

towards the land, while the land breeze occurs when the land's night-time temperature is less than the sea surface temperature and it is most common in winter and fall seasons (NOAA 2016). The sea breeze, which most often occurs in the warmer months of the year, would be stronger if the temperature difference between the land and the sea becomes significant (Ackerman 2006; NWS 2010). Experimental research has demonstrated that the sea and land breeze circulation has been a permanent feature of the Persian Gulf climate. However, its dimensions altered seasonally and diurnally (Zhu and Atkinson 2004). As can be seen on the map (Figure 2), the Persian Gulf and the Gulf of Oman are closely connected to each other. Careful examination of the hourly wind roses (in Figure 17) shows that the studied site is surely under the sea and land breeze circulation effect. As it is clear, from night to daytime, wind direction changes reversely. In addition, the monthly diagram of wind speed (Figure 14) and the seasonal production of wind power (Table 4) clearly indicate

that in summer, the effect of sea breeze in the studied site is more extensive than in winter.

### 3.4. Wind turbine energy production

In this part of the study, the energy productions of different small wind turbines were determined. The power curves of these wind turbines are depicted in Figure 23. All of the proposed wind turbines have stall control except the two studied Bergey wind turbines, which have pitch control. A hub-height of 15 m for all the proposed wind turbines was considered. Furthermore, the overall loss factor for all the studied wind turbines was considered to be 17.7% (Nedaei, Assareh, and Biglari 2014). Additionally by using the log law method which is described in Section 2.7.3 of this paper, the wind speed value at 15 m was estimated to be 3.52 m/s. The results of the energy production in Table 3 indicate that 'Proven 15' has the highest energy production of 20,096 kWh/yr and the highest capacity factor of 15.27%. In general, the capacity factor of the studied wind turbines in the investigated region ranged from 5.96% to 15.27%, while the energy production ranged from 673 to 20,096 kWh/yr. Moreover, it is assumed that the energy production for all studied wind turbines (in Table 3) is estimated for the same investigated geographical position.

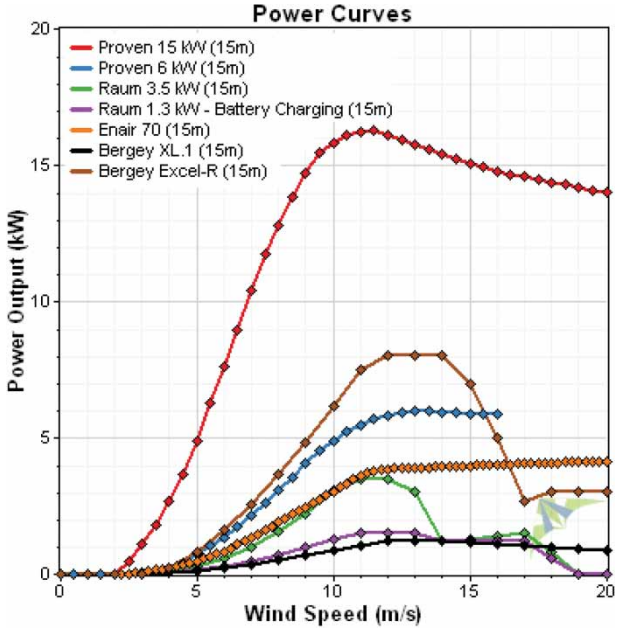


**Figure 23.** Power curve of different small wind turbines used in this research.

**Table 3.** Details of the selected wind turbines as well as their energy production (kWh/yr) and capacity factor (CF) in the investigated region.

| Turbine name | Rated power (kW) | Rotor diameter (m) | Energy production (kWh/yr) | Capacity factor (%) |
|---|---|---|---|---|
| Proven 15 | 15 | 9 | 20,096 | 15.27 |
| Raum 1.3 | 1.3 | 2.9 | 966 | 8.48 |
| Enair 70 | 3.5 | 4.1 | 2392 | 7.80 |
| Bergey XL.1 | 1 | 2.5 | 673 | 7.69 |
| Proven 6 | 6 | 5.5 | 3489 | 6.64 |
| Bergey Excel-R | 7.5 | 6.7 | 4129 | 6.28 |
| Raum 3.5 | 3.5 | 4 | 1826 | 5.96 |

**Table 4.** Seasonal production of a selected wind turbine (Proven 15).

| Seasons | Average energy production (kWh) |
|---|---|
| Spring | 2051.41 |
| Summer | 2141.42 |
| Autumn | 1654.66 |
| Winter | 1137.77 |

In addition, the seasonal production of wind energy for one of the selected wind turbines with the highest CF, 'Proven 15', is demonstrated in Table 4. It can be realised that the mean energy output in the warm seasons of the year is substantially more than the energy production in the cold seasons. It is evident that in the studied site, as the weather becomes colder, the energy production decreases considerably.

### 3.5. Economic evaluation of installing a selected small wind turbine in the studied area

In this study as it was elaborated in the previous section, most of the selected small wind turbines have a low calculated capacity factor (CF) and energy production due to poor wind potential of the studied region. The highest CF was observed for the wind turbine 'Proven 15' with the value of 15.27%. So this turbine was selected for an economic analysis in the studied region. For this purpose, Equations (28)–(31) are used to determine the cost of electricity in the studied region. The cost of a 15 kW Proven wind turbine is estimated to be $80,000 (Nedaei, Assareh, and Biglari 2014). Additionally we assume that other initial costs including installation, transportation, custom fee and grid integration are 40% of the turbine cost. Annual operation and maintenance costs plus the land rent amount to 6% of the turbine cost (Nedaei, Assareh, and Biglari 2014). The total installation cost of the wind turbine with 15 m hub-height is as follows:

$$80,000 \times \frac{40}{100} = \$32,000. \tag{31}$$

So, the total initial investment for the project is 80,000 + 32,000 = $112,000. The useful life of the system is assumed to be 20 years. Additionally the recent interest rate in Iran is considered to be 20% (Al-Monitor 2016). Thus, the capital recovery factor would be as follows:

$$\text{CRF} = \frac{0.20(1.2)^{20}}{(1.2)^{20} - 1} = 0.205. \tag{32}$$

Therefore, the cost of 1 kWh of electricity would be:

$$\text{UCE} = \frac{(112,000)(0.205 + 0.06)}{(8760)(15)(0.1527)} = \$1.479/\text{kWh}. \tag{33}$$

Based on a new research published by Elsevier (Fazelpour et al. 2015), currently wind farm owners in different locations of Iran such as Manjil and Binalood are selling electricity at the tariff rate of 0.18 $/kWh to the government. According to the above calculations (Equations (33)–(35)), it costs $1.479 for 1 kWh in the onshore investigated area which is $1.299 more than the market price. It became clear that both technically and economically the investigated area currently does not have sufficient wind power for electrical production. However, generally, it cannot be said that the studied area is not an appropriate place for harnessing

the wind energy. This area may have enough power for non-grid-connected mechanical applications, such as wind generators for water pumping. Additionally, the current work was a preliminary study for investigating the wind resource of southern onshore locations in Iran. Hence, we aim to continue the current research by focusing on the following issues:

(1) Installation of more meteorological masts in the southern onshore locations of Iran in order to evaluate the wind potential and direction for these regions. Accordingly it would be easier for policy-makers and planners to decide whether or not the southern onshore parts of Iran have enough wind potential for construction of onshore wind farms.
(2) Evaluation of water pumping potential in the studied site by using appropriate and modern wind turbines which require lower start-up wind speed would be one of the other challenges concerning the wind power utilisation in the investigated area.

## 4. Conclusion

The aim of this study was to evaluate the potential of onshore wind in the south of Iran along the Gulf of Oman. In order to specify the potential of wind in the investigated area, three numerical methods for estimating the Weibull parameters, that is, MLM, LSA (graphical method) and MM, have been compared to each other. It became clear that among all studied methods, MLM appeared to be the best algorithm for estimating the Weibull parameters ($c$ and $k$). Therefore, this method was employed to evaluate and estimate the distribution of wind speed, WPD and wind turbine energy production. Furthermore, the monthly as well as diurnal wind speed profile, turbulence intensity, surface roughness, wind direction and other wind speed characteristics were evaluated. Analysis of the surface roughness showed that the maximum surface roughness values are observed in the west direction from 270° to 330°. In addition, according to evaluation of TI, it is shown that the maximum peak values occurred in the direction sectors of 292.5° and 225° with a value of approximately 3.3. Moreover, the techno-economic evaluation of different small wind turbines showed that among all studied wind turbines, 'Proven 15' has the highest capacity factor (14.45%) and energy production (19,839 kWh/yr). According to the seasonal analysis of energy production, it became clear that in the warmer months of the year, the wind turbine energy production increases substantially.

The final results indicate that although the wind potential of the studied area is weak, it does not mean that it cannot be utilised. Nowadays luckily different research organisations around the world are trying to design new wind turbines to work in wind speeds as low as even 0.5 mph. Some of these wind turbines have been entered into the production process (Delft University 2014; Wind Power Authority 2015). On the other hand, non-grid-connected mechanical applications, such as wind generators for water pumping may also be suitable alternatives for poor wind conditions (Keyhani et al. 2010; Mostafaeipour et al. 2011). However, for the case of the investigated site, more research on this issue is required.

Accordingly, future work and research should be focused on the following issues and tasks:

(1) Installation of more meteorological masts along the Persian Gulf as well as the Gulf of Oman for precise assessment of onshore wind resources in the southern locations of Iran. Additionally, this methodology will be extended to evaluate all onshore locations of Iran including onshore regions of the Caspian Sea.
(2) Evaluation of water pumping potential by using appropriate and modern wind turbines which require lower start-up wind speed values.
(3) In order to precisely investigate the onshore wind power potential in the Gulf of Oman, assessing the sea and land breeze potential and evaluating the effect of sea breeze on wind regimes of coastal areas in Gulf of Oman are important aspects of WRA that must be carried out.

## Acknowledgment

The authors are grateful for the constructive and helpful comments provided by the reviewers and editors of the *International Journal of Ambient Energy*.

## Disclosure statement

No potential conflict of interest was reported by the authors.

## References

Abam, F. I., and O. S. Ohunakin. 2015. "Economics of Wind Energy Utilisation for Water Pumping and $CO_2$ Mitigation Potential in Niger Delta, Nigeria." *International Journal of Ambient Energy* 1–11.

Ackerman, D. S. 2006. *Sea and Land Breezes*. Wisconsin: University of Wisconsin.

Adaramola, M. S., M. Agelin-Chaab, and S. S. Paul. 2014. "Assessment of Wind Power Generation Along the Coast of Ghana." *Energy Conversion and Management* 77: 61–69.

Ahmed, S. 2011. *Wind Energy: Theory and Practice*. New Delhi: PHI Learning.

Akorede, M. F., M. I. Mohd Rashid, M. H. Sulaiman, N. B. Mohamed, and S. B. Ab Ghani. 2013. "Appraising the Viability of Wind Energy Conversion System in the Peninsular Malaysia." *Energy Conversion and Management* 76: 801–810.

Alamdari, P., O. Nematollahi, and M. Mirhosseini. 2012. "Assessment of Wind Energy in Iran: A Review." *Renewable and Sustainable Energy Reviews* 16 (1): 836–860.

Al-Monitor. 2016. The Pulse of the Middle East. "Iran Slashes Interest Rates to Boost Economy". Accessed January 2016. http://www.al-monitor.com/pulse/originals/2015/05/interest-rates-challenge-iran-economy.html.

Ammonit Measurement GmbH. 2015. Measurement Equipment for the Wind and Solar Industry. Accessed September 2015. http://www.ammonit.com/en.

Assareh, E., I. Poultangari, E. Tandis, and M. Nedaei. Forthcoming. "Optimizing the Wind Power Generation in Low Wind Speed Areas Using an Advanced Hybrid RBF Neural Network Coupled with the HGA-GSA Optimization Method." *Journal of Mechanical Science and Technology*, Accepted manuscript, Springer.

Ataei, A., M. Biglari, M. Nedaei, E. Assareh, J.-K. Choi, C. Yoo, and M. S. Adaramola. 2015a. "Techno-economic Feasibility Study of Autonomous Hybrid Wind and Solar Power Systems for Rural Areas in Iran, a Case Study in Moheydar Village." *Environmental Progress and Sustainable Energy* 34 (5): 1521–1527.

Ataei, A., M. Nedaei, R. Rashidi, and C. Yoo. 2015b. "Optimum Design of an Off-grid Hybrid Renewable Energy System for an Office Building." *Journal of Renewable and Sustainable Energy* 7 (5): 053123. doi:10.1063/1.4934659.

Biglari, M., E. Assareh, M. Nedaei, and I. Poultangari. 2013. "An Initial Evaluation of Wind Resource in the Port of Chabahar in South East of Iran." *Global Journal of Science and Engineering Technology* 2 (14): 142–148.

Boudia, S. M., A. Benmansour, N. Ghellai, M. Benmedjahed, and M. A. Tabet Hellal. 2013. "Temporal Assessment of Wind Energy Resource at Four Locations in Algerian Sahara." *Energy Conversion and Management* 76: 654–664.

Chang, T. P. 2011. "Performance Comparison of Six Numerical Methods in Estimating Weibull Parameters for Wind Energy Application." *Applied Energy* 88 (1): 272–282.

Cook, N. J. 1986. *Designers Guide to Wind Loading of Building Structures. Part 1*. Oxford: Butterworth-Heinemann.

Delft University of Technology. 2014. Duwind Section. Accessed December 11, 2014. http://www.duwind.tudelft.nl.

Fazelpour, F., N. Soltani, S. Soltani, and M. A. Rosen. 2015. "Assessment of Wind Energy Potential and Economics in the North-western Iranian Cities of Tabriz and Ardabil." *Renewable and Sustainable Energy Reviews* 45: 87–99.

Google Earth. 2015. Accessed April 11, 2015. www.maps.google.com.

Gualtieri, G. 2015. "Surface Turbulence Intensity as a Predictor of Extrapolated Wind Resource to the Turbine Hub Height." *Renewable Energy* 78: 68–81.

Jain, P. 2010. *Wind Energy Engineering*. New York: McGraw Hill Professional.

Kandpal, T. C., and H. P. Garg. 2003. *Financial Evaluation of Renewable Energy Technologies*. New Delhi: MacMillam.

Keyhani, A., M. Ghasemi-Varnamkhasti, M. Khanali, and R. Abbaszadeh. 2010. "An Assessment of Wind Energy Potential as a Power Generation Source in the Capital of Iran, Tehran." *Energy* 35 (1): 188–201.

Khahro, S. F., K. Tabbassum, A. M. Soomro, L. Dong, and X. Liao. 2013. "Evaluation of Wind Power Production Prospective and Weibull Parameter Estimation Methods for Babaurband, Sindh Pakistan." *Energy Conversion and Management* 78: 956–967.

Kose, F., M. H. Aksoy, and M. Ozgoren. 2014. "An Assessment of Wind Energy Potential to Meet Electricity Demand and Economic Feasibility in Konya, Turkey." *International Journal of Green Energy* 11 (6): 559–576.

Mirhosseini, M., F. Sharifi, and A. Sedaghat. 2011. "Assessing the Wind Energy Potential Locations in Province of Semnan in Iran." *Renewable and Sustainable Energy Reviews* 15 (1): 449–459.

Mostafaeipour, A., A. Sedaghat, A. A. Dehghan-Niri, and V. Kalantar. 2011. "Wind Energy Feasibility Study for City of Shahrbabak in Iran." *Renewable and Sustainable Energy Reviews* 15 (6): 2545–2556.

Nedaei, M. 2014. "Wind Resource Assessment in Hormozgan Province in Iran." *International Journal of Sustainable Energy* 33 (3): 650–694.

Nedaei, M., E. Assareh, and M. Biglari. 2014. "An Extensive Evaluation of Wind Resource Using New Methods and Strategies for Development and Utilizing Wind Power in Mahshahr Station in Iran." *Energy Conversion and Management* 81: 475–503.

Nedaei, M., A. Ataei, C. Yoo, J. K. Choi, and E. Assareh. 2016. "The Potential of Wind for Energy Production and Water Pumping in Iran, Saravan County." *Distributed Generation & Alternative Energy Journal* 31(1): 7–26.

NOAA (National Oceanic and Atmospheric Administration). 2016. Accessed January 2016. http://oceanservice.noaa.gov/education/pd/oceans_weather_climate and http://oceanservice.noaa.gov/education/pd/oceans_weather_climate/media/sea_and_land_breeze.swf.

Nojedehi, P., M. Heidari, A. Ataei, M. Nedaei, and E. Kurdestani. 2016. "Environmental Assessment of Energy Production from Landfill Gas Plants by Using Long-range Energy Alternative Planning (LEAP) and IPCC Methane Estimation Methods: A Case Study of Tehran." *Sustainable Energy Technologies and Assessments* 16: 33–42.

NWS (National Weather Service). 2010. The Sea Breeze. Accessed January 2016. http://www.srh.weather.gov/srh/jetstream/ocean/seabreezes.htm.

Rocha, P. A. C., R. C. de Sousa, C. F. de Andrade, and M. E. V. da Silva. 2012. "Comparison of Seven Numerical Methods for Determining Weibull Parameters for Wind Energy Generation in the Northeast Region of Brazil." *Applied Energy* 89 (1): 395–400.

Seguro, J. V., and T. W. Lambert. 2000. "Modern Estimation of the Parameters of the Weibull Wind Speed Distribution for Wind Energy Analysis." *Journal of Wind Engineering and Industrial Aerodynamics* 85: 75–84.

SUNA. 2015. Renewable Energy Organization of Iran. Accessed April 11, 2015. www.suna.org.ir.

Sunderland, K. M., G. Mills, and M. F. Conlon. 2013. "Estimating the Wind Resource in an Urban Area: A Case Study of Micro-wind Generation Potential in Dublin, Ireland." *Journal of Wind Engineering and Industrial Aerodynamics* 118: 44–53.

Theodor Friedrichs & CO. 2016. Accessed April 20, 2016. http://www.th-friedrichs.de/en/home.

WINDSENSOR. 2015. Meteorological Instruments Company. Accessed September, 2015. http://www.windsensor.dk.

Windographer™. 2015. Wind Resource Assessment Tool. Accessed December 2015. http://www.windographer.com.

Wind Power Authority. 2015. Accessed February 11, 2015. http://windpowerauthority.com/top-5-low-speed-wind-turbines.

WMI. 2015. Wind Measurement International. Accessed September 2015. http://www.windmi.com.

Wua, J., J. Wanga, and D. Chib. 2013. "Wind Energy Potential Assessment for the Site of Inner Mongolia in China." *Renewable and Sustainable Energy Reviews* 21: 215–228.

WWEA (World Wind Energy Association). 2015a. *New Record in Worldwide Wind Installations*. Accessed January 10, 2016. http://www.wwindea.org/new-record-in-worldwide-wind-installations/.

WWEA (World Wind Energy Association). 2015b. *World Wind Energy Quarterly Bulletin 2015 (Special issue)*. Accessed January 10, 2016. http://www.wwindea.org/download/wwea_quaterly_bulletin/Bulletin2015.pdf.

Zhu, M., and B. W. Atkinson. 2004. "Observed and Modelled Climatology of the Land–sea Breeze Circulation Over the Persian Gulf." *International Journal of Climatology* 24: 883–905.